Leg-by-leg Bearings-Only Target Motion Analysis Without Observer Maneuver

CLAUDE JAUFFRET
DENIS PILLON
ANNIE-CLAUDE PIGNOL

In a previous paper [7], the problem of bearings-only tracking of targets whose trajectory is composed of two legs from a non-maneuvering observer was addressed and the maximum likelihood estimate (MLE) proposed. We named it bearings-only maneuvering target motion analysis (BOMTMA). Recently in [9], we proposed another estimate based on leg-by-leg tracking and compare its performance to the MLE. We give here the extended version of [9], together with some comparison between the conventional bearings-only target motion analysis (BOTMA) and the BOMTMA.

Manuscript received November 12, 2009; revised October 27, 2010; released for publication February 08, 2011.

Refereeing of this contribution was handled by Huimin Chen.

Authors' addresses: C. Jauffret, Université Sud Toulon-Var, CNRS, IM2NP (UMR 6242), Bâtiment X, BP 132, 83957 La Garde Cedex, France, Email: (jauffret@univ-tln.fr); D. Pillon, Thales Underwater Systems, 525 Route des Dolines, 06903 Sophia-Antipolis, France, Email: (denis.pillon@fr.thalesgroup.com); A. C. Pignol, Université Sud Toulon-Var, CNRS, IM2NP (UMR 6242), Bâtiment X, BP 132, 83957 La Garde Cedex, France, Email: (pignol@univ-tln.fr).

1. INTRODUCTION

The conventional problem of bearings-only target motion analysis consists of estimating the trajectory of a target (or source) whose velocity is constant during the period of measurement [13]. This requires an efficient maneuver of the observer to guarantee observability [6][12] and to obtain an accurate estimate [11][15]. In a recent paper [7], we proved that, conversely, if the observer has a constant velocity and the source changes its heading (so its trajectory is composed of two legs at constant speed—see Fig. 5), then, subject to a condition on velocity vectors of the two mobiles, the source is observable. For this problem, called bearings-only maneuvering target motion analysis (BOMTMA), we proposed the maximum likelihood estimate (MLE) and compared its performance with the Cramér-Rao lower bound (CRLB), revealing that this estimate is relatively efficient. The major criticisms are

1) The operator must wait until the source has changed its heading to run the computation of the estimate.
2) The computation by a numerical routine needs a "good guess" (to reduce the risk of converging toward a local minimum).
3) The computation takes time.

In this paper, we propose a new approach to this problem which consists of estimating what is observable during the first leg of the source, then during the second one, and finally of fusing these two estimated state vectors to obtain an estimate of the source trajectory. Note that in the classic BOTMA, the leg-by-leg approach has been employed for the same reasons [2][14][16]. We will assume that the maneuver time is known, hence we will not address the problem of detecting the maneuver (see [5] and [17] for this topic).

The paper is composed of three main sections:

- In Section 2, we present the problem of target motion analysis (TMA) when neither the source nor the observer maneuvers.
- A new bearings-only maneuvering target motion analysis by a non-maneuvering observer is proposed in Section 3.
- In Section 4, some examples are provided to compare respective performances of BOTMA and BOMTMA, in terms of estimated range accuracy.

2. PROBLEM FORMULATION WHEN NEITHER THE SOURCE NOR THE OBSERVER MANEUVERS

We consider in this section the case where the source and the observer are moving in the same plane with their own constant velocity vectors (see Fig. 1).

2.1. Measurement Equation and Trajectory Model

Consider a source and a passive observer (also called own ship). From here on, the subscript S is used to

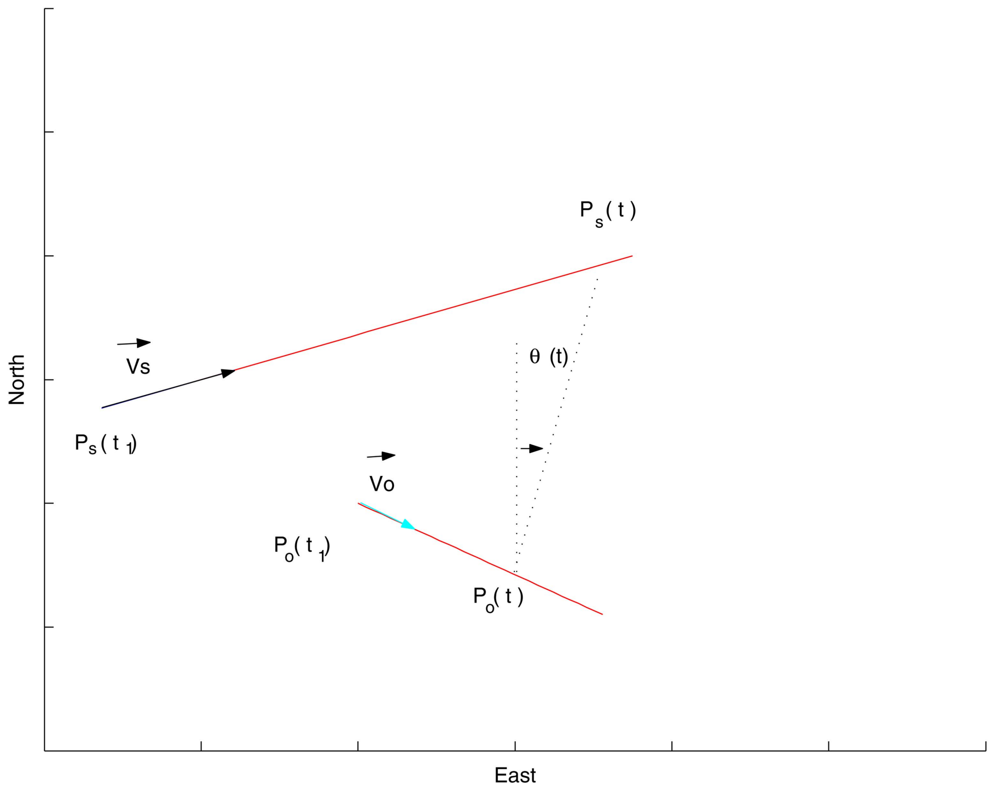

Fig. 1. Example of observer and source trajectories.

represent source quantities and O to represent observer quantities.

At time t, the respective location vectors of the source and of the observer are $P_S(t) = [x_S(t)\ \ y_S(t)]^{\mathrm{T}}$ and $P_O(t) = [x_O(t)\ \ y_O(t)]^{\mathrm{T}}$ relative to a Cartesian coordinate system. Similarly, the vectors $V_S = [\dot{x}_S\ \ \dot{y}_S]^{\mathrm{T}}$ and $V_O = [\dot{x}_O\ \ \dot{y}_O]^{\mathrm{T}}$ denote the source and own ship velocity vectors, respectively. We define also the relative velocity vector of the source w.r.t. the observer as $V_R = V_S - V_O$. The corresponding speeds and headings (or courses) are denoted v_S, v_O, v_R, c_S, c_O and c_R.

At time t_k, the observer measures the azimuth of the line of sight in which it detects the source:

$$\beta_k = \operatorname{atan}\left[\frac{x_S(t_k) - x_O(t_k)}{y_S(t_k) - y_O(t_k)}\right] + \varepsilon_k \qquad (1)$$

where ε_k is assumed to be a zero-mean Gaussian random noise of variance σ_k^2.

The BOTMA aims to estimate

$$X_S = [x_S(t^*)\ \ y_S(t^*)\ \ \dot{x}_S\ \ \dot{y}_S]^{\mathrm{T}}$$

from the collected measurement set $\{\beta_1, \beta_2, \ldots, \beta_N\}$ provided observability is guaranteed (t^* is an arbitrary reference time). The vector $X_O = [x_O(t^*)\ \ y_O(t^*)\ \ \dot{x}_O\ \ \dot{y}_O]^{\mathrm{T}}$ is known. It is well known that if the observer does not maneuver or if its maneuver is ambiguous (see [6] and [10]), then the vector X_S is not observable. In the coming paragraph, we explore the situations where the observer keeps its velocity vector during the scenario.

2.2. The Set of Homothetic Trajectories

The trajectory of a vehicle moving at a constant velocity vector $[\dot{x}\ \ \dot{y}]^{\mathrm{T}}$ is described by the following classic equations:

$$\begin{aligned} x(t) &= x(t^*) + (t - t^*)\dot{x} \\ y(t) &= y(t^*) + (t - t^*)\dot{y}. \end{aligned} \qquad (2)$$

Such a trajectory is hence defined by the vector $X = [x(t^*)\ \ y(t^*)\ \ \dot{x}\ \ \dot{y}]^{\mathrm{T}}$.

The equation of the noise-free bearings being $\theta(t) = \operatorname{atan}[(x_S(t) - x_O(t))/(y_S(t) - y_O(t))]$, it is straightforward to check that the set of trajectories producing the same noise-free-bearings from the observer is

$$\Lambda = \{X(\lambda) = \lambda(X_S - X_O) + X_O,\ \text{for}\ \lambda > 0\}.$$

If $\theta(t)$ is not constant, there is no other trajectory set that generates the same noise-free data when the source and observer are moving at constant velocity vectors [10]. From now on, we will assume that $\theta(t)$ is not constant.

Note that the vector

$$X(\lambda) = [x_1(\lambda)\quad x_2(\lambda)\quad x_3(\lambda)\quad x_4(\lambda)]^{\mathrm{T}}$$

defines a λ-homothetic trajectory (in particular, $X(1) = X_S$).

It follows that X_S is not observable from the bearing measured by the observer. In short, in this context, the BOTMA is impossible. We can however estimate a parameter (or a state vector) that characterizes Λ. We call the estimation of this parameter (or any equivalent parameter) partial bearing-only target motion analysis (see Subsection 2.4).

The previous set Λ can be characterized by any of its elements $X(\lambda)$. At any $X(\lambda)$ of Λ, there is a corresponding unique three dimensional vector $Y = [y_1 \ \ y_2 \ \ y_3]^{\mathrm{T}}$ defined by

$$y_1 = \operatorname{atan}\left[\frac{x_1(\lambda) - x_O(t^*)}{x_2(\lambda) - y_O(t^*)}\right]$$
$$y_2 = \frac{\sqrt{(x_3(\lambda) - \dot{x}_O)^2 + (x_4(\lambda) - \dot{y}_O)^2}}{\sqrt{[x_1(\lambda) - x_O(t^*)]^2 + [x_2(\lambda) - y_O(t^*)]^2}} \tag{3}$$
$$y_3 = \operatorname{atan}\left[\frac{x_3(\lambda) - \dot{x}_O}{x_4(\lambda) - \dot{y}_O}\right].$$

Indeed, the coordinates of Y are independent of λ:

$$y_1 = \theta(t^*), \qquad y_2 = \frac{v_R}{\rho_a(t^*)} \qquad \text{and} \qquad y_3 = c_R$$

where $\rho_a(t^*)$ is the actual range between the source and the observer at time t^* (see [6, 7]). Note that because $\theta(t)$ is not constant, we have $V_S \neq V_O$, hence $y_2 > 0$.

We can plot the set of homothetic trajectories Λ using the graphs of the two functions

$$\rho \mapsto v(\rho) = \sqrt{(\rho y_2 \sin y_3 + \dot{x}_O)^2 + (\rho y_2 \cos y_3 + \dot{y}_O)^2} \tag{4a}$$

$$\rho \mapsto c(\rho) = \operatorname{atan}\left[\frac{\rho y_2 \sin y_3 + \dot{x}_O}{\rho y_2 \cos y_3 + \dot{y}_O}\right] \tag{4b}$$

where $[v(\rho) \ \ c(\rho)]^{\mathrm{T}}$ are the polar coordinates of the velocity vector of any source of Λ at a distance ρ (≥ 0) at time t^* (the corresponding λ is equal to $\rho/\rho_a(t^*)$). Note that $v(\rho_a(t^*)) = v_S$ and $c(\rho_a(t^*)) = c_S$.

We insist on the fact that

1) any element of Λ allows us to construct the vector Y (see Eq. (3));

2) conversely, the vector Y allows us to construct any element of Λ, thank to the following equation

$$X\left(\frac{\rho}{\rho_a(t^*)}\right) = \frac{\rho}{\rho_a(t^*)}(X_S - X_O) + X_O$$
$$= \frac{\rho}{\rho_a(t^*)}\begin{bmatrix} \rho_a(t^*)\sin y_1 \\ \rho_a(t^*)\cos y_1 \\ \rho_a(t^*) y_2 \sin y_3 \\ \rho_a(t^*) y_2 \cos y_3 \end{bmatrix} + X_O.$$

This equivalence between Y and Λ is the fundamental property of the partial bearings-only TMA which will be developed in Section 3. As a consequence, we can choose the vector Y as well any vector in Λ. The choice of a state vector must be guided by simplicity.

Because it is expressed in polar coordinates, Y is subject to a constraint: $y_2 > 0$, whereas any vector of Λ (expressed in Cartesian coordinates) is not. So, from the point of view of the estimation, choosing a particular vector of Λ as state vector is more convenient. A way to "stay" in Λ is to fix one coordinate of a 4-dimensional vector X and "adjust" the remained coordinates to Y:

For example, if we fix the first coordinate of an particular element of Λ to the value x_{fix}, the corresponding λ will be $\lambda = (x_{\text{fix}} - x_O(t^*))/(x_S(t^*) - x_O(t^*))$; however, we must choose x_{fix} such that λ be positive. This will help us in Subsection 2.4.

2.3. Properties of $v(\rho)$ and $c(\rho)$

First of all, we note that $v(0)$ and $c(0)$ are equal to the observer's speed and heading, respectively. This corresponds to the degenerate case where the observer and the source are located at the same position.

2.3.1. Study of $v_S(\rho)$

Let us compute its derivative w.r.t. ρ.

$$\frac{d}{d\rho}v(\rho) = \frac{1}{v(\rho)}[(\rho y_2 \sin y_3 + \dot{x}_O) y_2 \sin y_3 + (\rho y_2 \cos y_3 + \dot{y}_O) y_2 \cos y_3]$$
$$= \frac{y_2}{v(\rho)}[\rho y_2 + \dot{x}_O \sin y_3 + \dot{y}_O \cos y_3]$$
$$= \frac{y_2}{v(\rho)}\left[\rho y_2 + \frac{1}{v_R} V_O^{\mathrm{T}}(V_S - V_O)\right].$$

The sign of this derivative is hence the sign of $\rho y_2 + \dot{x}_O \sin y_3 + \dot{y}_O \cos y_3$. It is equal to 0 when $\rho = -(1/y_2 v_R) \cdot V_O^{\mathrm{T}}(V_S - V_O)$.

If $V_O^{\mathrm{T}}(V_S - V_O) \geq 0$ or equivalently $V_O^{\mathrm{T}} V_S \geq v_O^2$, the function $v_S(\rho)$ is injective, i.e. the mapping $\rho \mapsto v(\rho)$ satisfies the one-to-one condition.

We draw two other conclusions:

1) The one-to-one condition holds if and only if $\dot{x}_S \sin c_O + \dot{y}_S \cos c_O \geq v_O$.

2) The set of source's velocity vectors V_S satisfying the one-to-one condition of the speed is

$$\left\{ V_S = \alpha \begin{bmatrix} \sin c_O \\ \cos c_O \end{bmatrix} - \beta \begin{bmatrix} \cos c_O \\ \sin c_O \end{bmatrix}, \quad \text{for any } \alpha \geq v_O \text{ (no condition for } \beta) \text{ and } V_S \neq V_O \right\}$$

Note that α and β that help define the above set are dummy variables.

2.3.2. Study of $c(\rho)$

First of all, note that $c(\rho)$ goes to c_R when $\rho \to \infty$.

A basic computation yields

$$\frac{d}{d\rho}c(\rho) = \frac{y_2(\dot{y}_O \sin y_3 - \dot{x}_O \cos y_3)}{v^2(\rho)}$$

which has the same sign as

$$v_R(\dot{y}_O \sin y_3 - \dot{x}_O \cos y_3) = -\det[V_O, (V_S - V_O)],$$

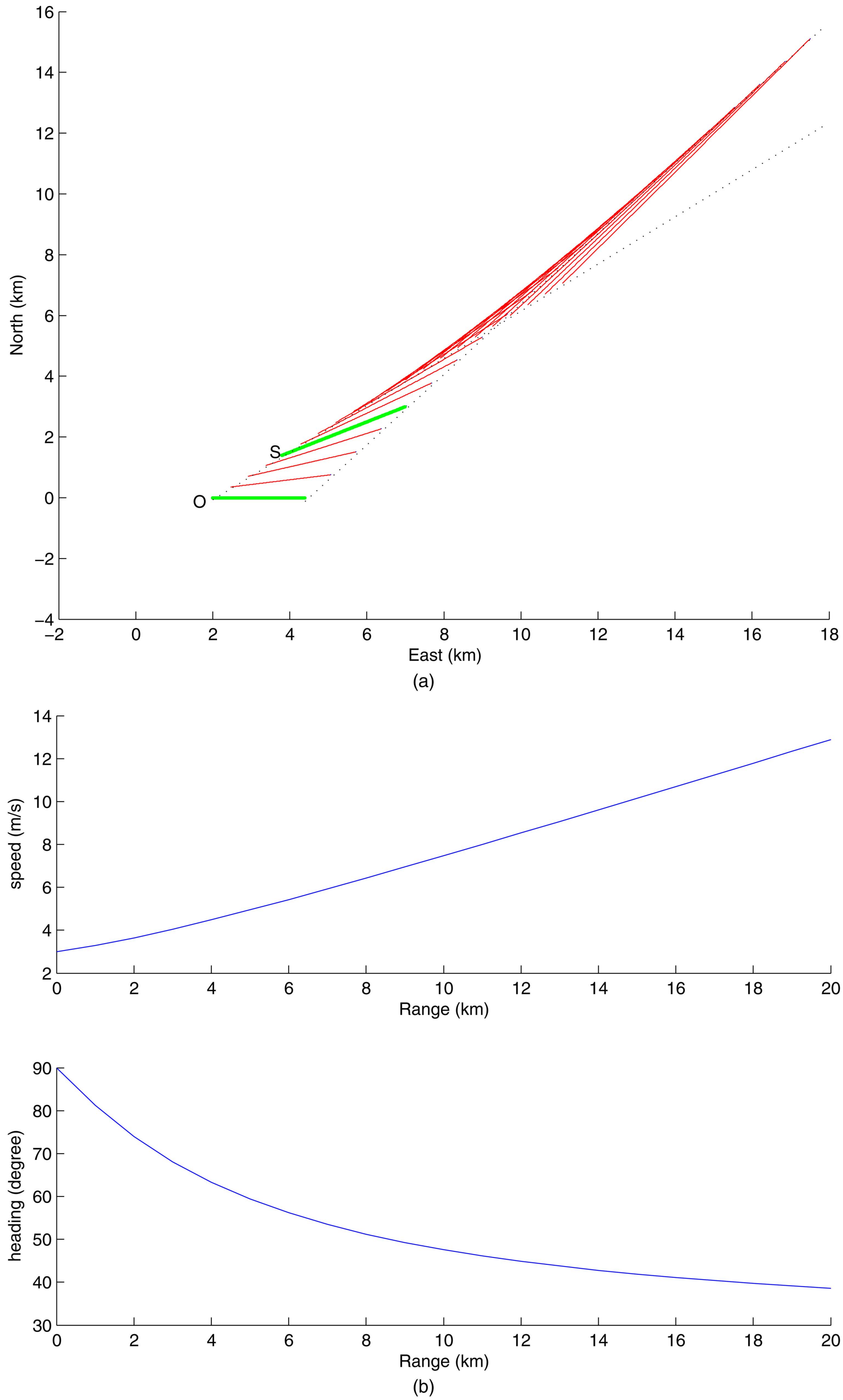

Fig. 2. (a) Some elements of Λ. (b) The corresponding speed and heading graphs.

which is independent of ρ. Hence the mapping $\rho \mapsto c(\rho)$ is monotonic while the mapping $\rho \mapsto v(\rho)$ can be not.

Fig. 2 gives an example of an increasing speed function for $V_O = [3\ \ 0]^{\mathrm{T}}$ (m/s) and $V_S = [4\ \ 2]^{\mathrm{T}}$ (m/s) corresponding to $(\alpha, \beta) = (4, 2)$; the initial positions are $P_S(t_0) = [3.8\ \ 1.4]^{\mathrm{T}}$ (km) and $P_O(t_0) = [2\ \ 0]^{\mathrm{T}}$ (km). Note that the condition $\dot{x}_S \sin c_O + \dot{y}_S \cos c_O \geq v_O$ is satisfied. In Fig. 2(a), letters O and S denote the initial position

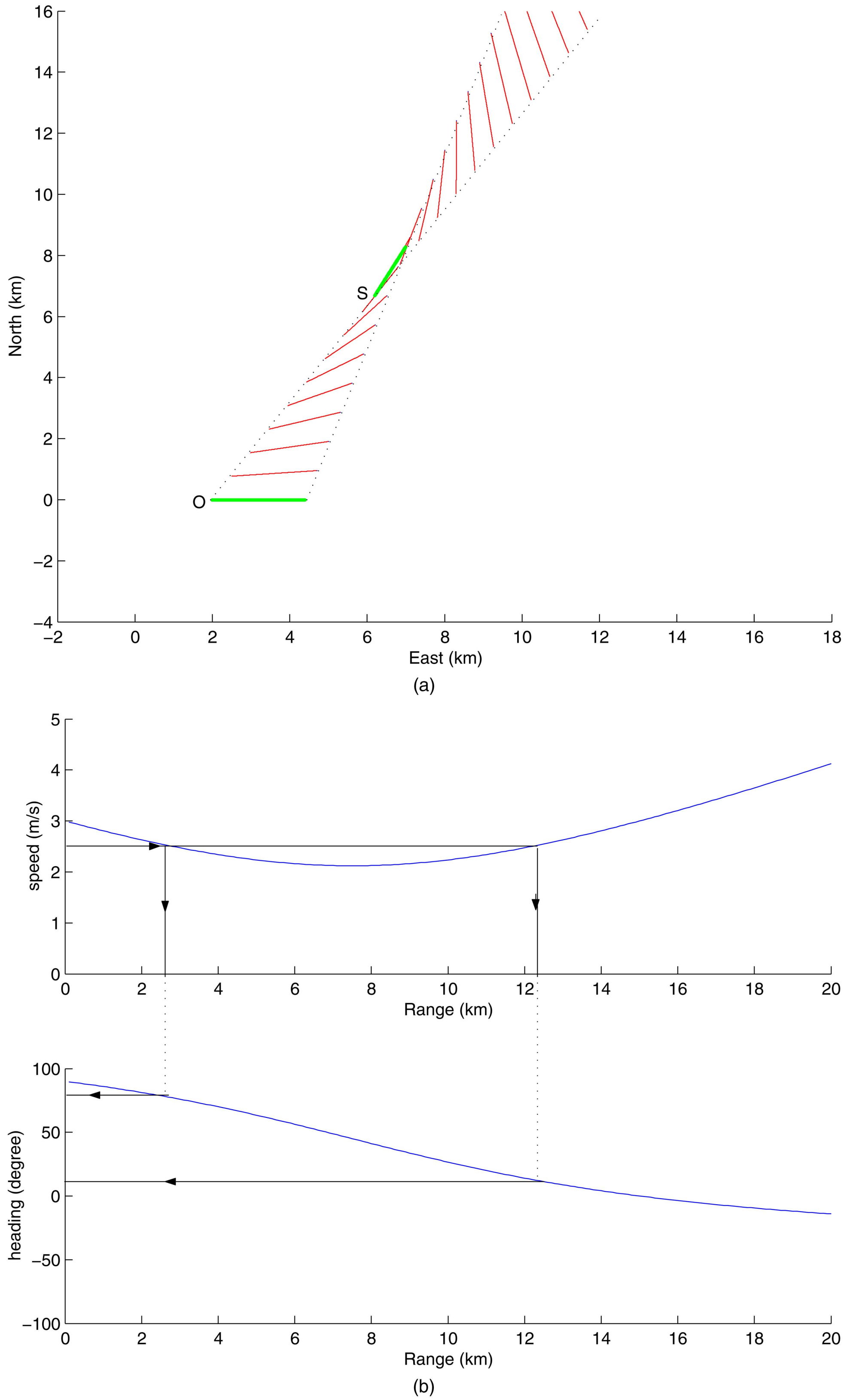

Fig. 3. (a) Some elements of Λ. (b) The corresponding speed and the heading graphs.

of the observer and that of the actual source and several homothetic solutions. Fig. 2(b) depicts $\rho \mapsto v(\rho)$ and $\rho \mapsto c(\rho)$; the small circles correspond to the actual speed and heading.

Fig. 3 illustrates the case of a non-monotonic speed function for $V_O = [3\ \ 0]^T$ (m/s) and $V_S = [1\ \ 2]^T$ (m/s) corresponding to $(\alpha, \beta) = (1, 2)$. The initial positions are $P_S(t_0) = [6.2\ \ 6.7]^T$ (km) and $P_O(t_0) = [2\ \ 0]^T$ (km). Here, the condition $\dot{x}_S \sin c_O + \dot{y}_S \cos c_O \geq v_O$ is violated.

In this case, due to the non-monotony of the mapping $\rho \mapsto v(\rho)$, a speed v would yield two corresponding estimated ranges and courses as shown in Fig. 3(b).

2.4. Estimation of the Set of Homothetic Trajectories (partial bearings-only TMA)

The available measured bearings $(\beta_1, \beta_2, \ldots, \beta_N)$ are taken at times $(t_1, t_2, \ldots, t_N)$. Without loss of generality, we choose $t^* = t_N$. Assuming the covariance matrix of the random vector $(\varepsilon_1 \ \ \varepsilon_2 \cdots \varepsilon_N)^{\mathrm{T}}$ to be diagonal, the log-likelihood function to be maximized is proportional to the least squares criterion. The vector Y or any vector in Λ can be chosen as state vector. Because of the simplicity of use of Cartesian coordinates, we propose to estimate a particular element of Λ by fixing its first coordinate x_1 to $\bar{\rho}\sin\beta_N + x_O(t_N)$ for convenience, $\bar{\rho}$ being arbitrarily chosen. We call it X. So we only have to compute the last three coordinates of $X = [\bar{\rho}\sin\beta_N + x_O(t_N) \ \ y \ \ \dot{x} \ \ \dot{y}]^{\mathrm{T}}$ for which the criterion $C(X) = \sum_{k=1}^{N}(1/\sigma_k^2)[\beta_k - \theta_k(X)]^2$ is minimal.

The Gauss-Newton method [3] is used for the minimization, initialized at

$$X_{\text{init}} = \begin{bmatrix} \bar{\rho}\sin\beta_N + x_O(t_N) \\ \bar{\rho}\cos\beta_N + y_O(t_N) \\ \dfrac{\bar{\rho}\sin\beta_N + x_O(t_N) - \bar{\rho}\sin\beta_1 - x_O(t_1)}{t_N - t_1} \\ \dfrac{\bar{\rho}\cos\beta_N + x_O(t_N) - \bar{\rho}\cos\beta_1 - x_O(t_1)}{t_N - t_1} \end{bmatrix}.$$

As pointed out previously, the maximum likelihood estimate $\hat{X}$ allows us to construct the set of estimated homothetic trajectories presented as the graphs of the pair of functions

$$\rho \mapsto \hat{v}(\rho) = \sqrt{(\rho\hat{y}_2 \sin\hat{y}_3 + \dot{x}_O)^2 + (\rho\hat{y}_2\cos\hat{y}_3 + \dot{y}_O)^2} \tag{5a}$$

$$\rho \mapsto \hat{c}(\rho) = \operatorname{atan}\left[\frac{\rho\hat{y}_2 \sin\hat{y}_3 + \dot{x}_O}{\rho\hat{y}_2\cos\hat{y}_3 + \dot{y}_O}\right] \tag{5b}$$

where $\hat{Y} = [\hat{y}_1 \ \ \hat{y}_2 \ \ \hat{y}_3]^{\mathrm{T}}$ is the vector corresponding to $\hat{X}$ (with (3)).

The behavior of the estimator $\hat{X}$ has been evaluated for the following scenario: given a coordinate system, the initial location of the source is $[1000 \ \ 2300]^{\mathrm{T}}$ (m) with a velocity vector of $[1 \ \ 1.5]^{\mathrm{T}}$ (m/s). The observer starts from $[0 \ \ 0]^{\mathrm{T}}$ (m) with a velocity vector $[1 \ \ 0]^{\mathrm{T}}$ (m/s). The number of measurements is $N = 450$, the time t_k is equal to $k \times \Delta t$, with $\Delta t = 4$ s. The time of reference is chosen to be t_N. The standard deviation of the measurements is 1°. The final range is 5,099 m. For the initialization of the Gauss-Newton method, we have chosen $\bar{\rho} = 20$ km.

Fig. 4 depicts an example of a 500-run Monte-Carlo simulation: the 500 graphs are plotted in grey, while the graphs of the functions $v(\rho)$ and $c(\rho)$ are in black, together with the 95% confidence bands (deduced from the CRLB). Detail of the computation of these bands is given in the Appendix.

3. LEG-BY-LEG BOMTMA

3.1. Problem Formulation

Suppose now that the trajectory of the source is composed of two legs at constant speed (cf. Fig. 5): the first leg starts at t_1 and finishes at time t_M (assumed to be known). Similarly, the second leg starts at t_M and finishes at t_K. This model of trajectory is simple, but it has been widely adopted in the past, especially in submarine environment (see [1] pp. 175–176 and [4]). The time of the maneuver is assumed to be known; in reality, it has to be estimated, for example by a sequential test; this point, which is out of the scope of this paper, has been addressed in [8]. Such a trajectory is hence parameterized by the vector $Z = [x_S(t_K) \ \ y_S(t_K) \ \ v_S \ \ c_{S,1} \ \ c_{S,2}]^{\mathrm{T}}$ (coordinates of position at time t_K, speed, courses of the first and of second leg). Provided that $V_O^{\mathrm{T}}(V_{S,1} - V_{S,2}) \neq 0$ (observability condition-see its proof in [7]), the entire source trajectory is observable. For this problem, we proposed the maximum likelihood estimate in [7].

We propose here another estimate denoted $\tilde{Z}$ the principle of which is as follows: First, we compute, for leg #1, the estimate

$$\hat{X}_1 = [\bar{\rho}\sin\beta_M + x_O(t_M) \quad \hat{y}_1 \quad \hat{\dot{x}}_1 \quad \hat{\dot{y}}_1]^{\mathrm{T}}$$

and for leg #2, the estimate

$$\hat{X}_2 = [\bar{\rho}\sin\beta_M + x_O(t_M) \quad \hat{y}_2 \quad \hat{\dot{x}}_2 \quad \hat{\dot{y}}_2]^{\mathrm{T}}$$

with the common reference time t_M and after having fixed their respective first coordinates to a common value, say $\bar{\rho}\sin\beta_M + x_O(t_M)$. These estimates are computed following the partial BO-TMA principle as presented in Section 2.4. Second, we compute the two homothetic estimates, $\mu(\hat{X}_1 - X_O) + X_O$ for the first leg and $\mu(\hat{X}_2 - X_O) + X_O$ for the second, such that the estimated velocities on each leg are equal, i.e.

$$\|\mu(\hat{V}_1 - V_O) + V_O\| = \|\mu(\hat{V}_2 - V_O) + V_O\| \tag{6}$$

with $\hat{V}_1 = [\hat{\dot{x}}_1 \ \ \hat{\dot{y}}_1]^{\mathrm{T}}$ and $\hat{V}_2 = [\hat{\dot{x}}_2 \ \ \hat{\dot{y}}_2]^{\mathrm{T}}$ in order to satisfy the constraint (6) (which is the strong assumptions of the BOMTMA). The solution of (6), denoted $\tilde{\mu}$, and equal to

$$\tilde{\mu} = -\frac{2(\hat{V}_1 - \hat{V}_2)^{\mathrm{T}}V_O}{(\|\hat{V}_1\|^2 - \|\hat{V}_2\|^2 - 2(\hat{V}_1 - \hat{V}_2)^{\mathrm{T}}V_O)}$$

allows us to compute the corresponding homothetic estimates on each leg

$$\tilde{X}_1 = \tilde{\mu}(\hat{X}_1 - X_O) + X_O = [\tilde{x}_1 \quad \tilde{y}_1 \quad \tilde{\dot{x}}_1 \quad \tilde{\dot{y}}_1]^{\mathrm{T}}$$

$$\tilde{X}_2 = \tilde{\mu}(\hat{X}_2 - X_O) + X_O = [\tilde{x}_2 \quad \tilde{y}_2 \quad \tilde{\dot{x}}_2 \quad \tilde{\dot{y}}_2]$$

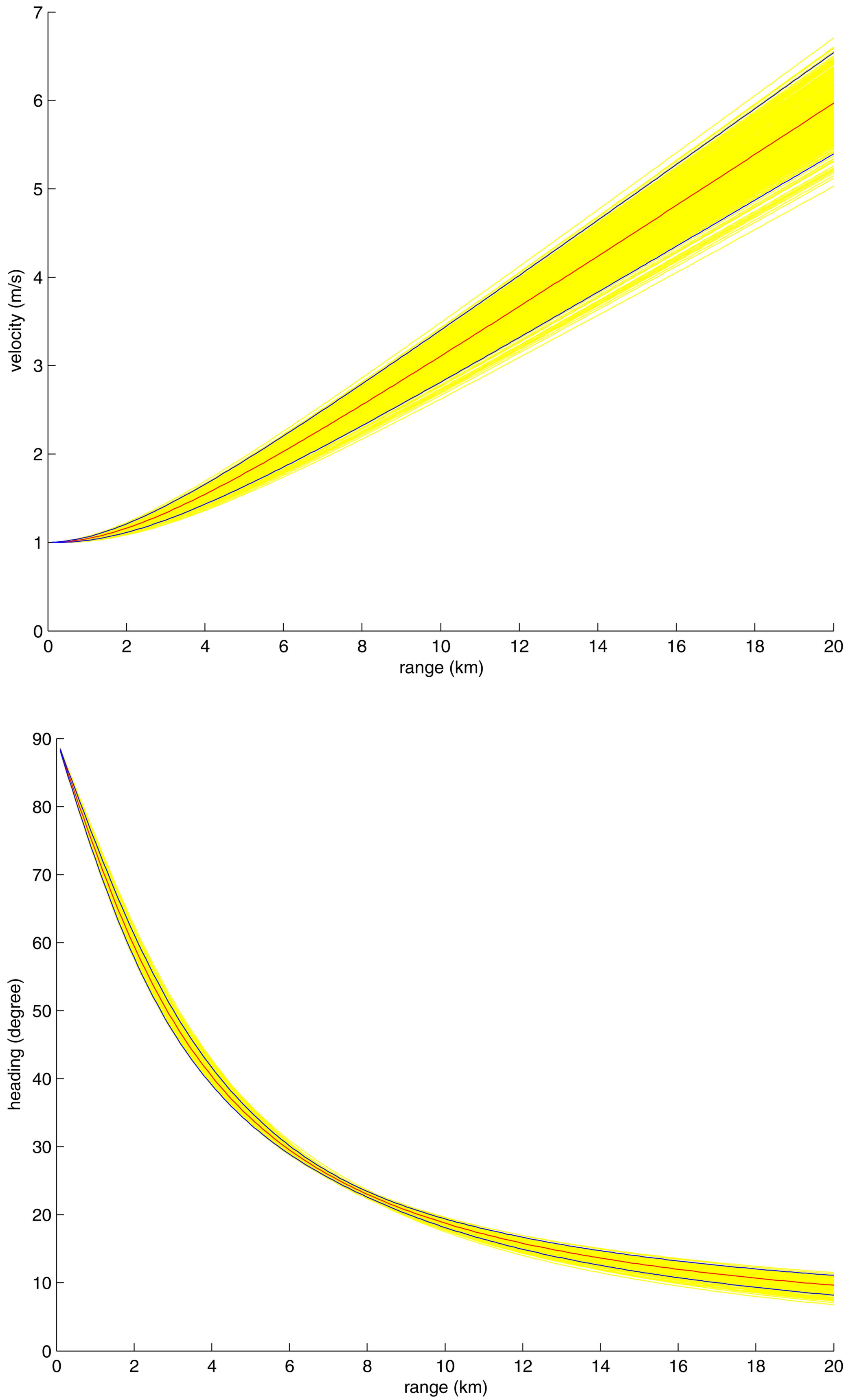

Fig. 4. Results of 500 Monte-Carlo runs (on left $\hat{v}(\rho)$, and on right $\hat{c}(\rho)$).

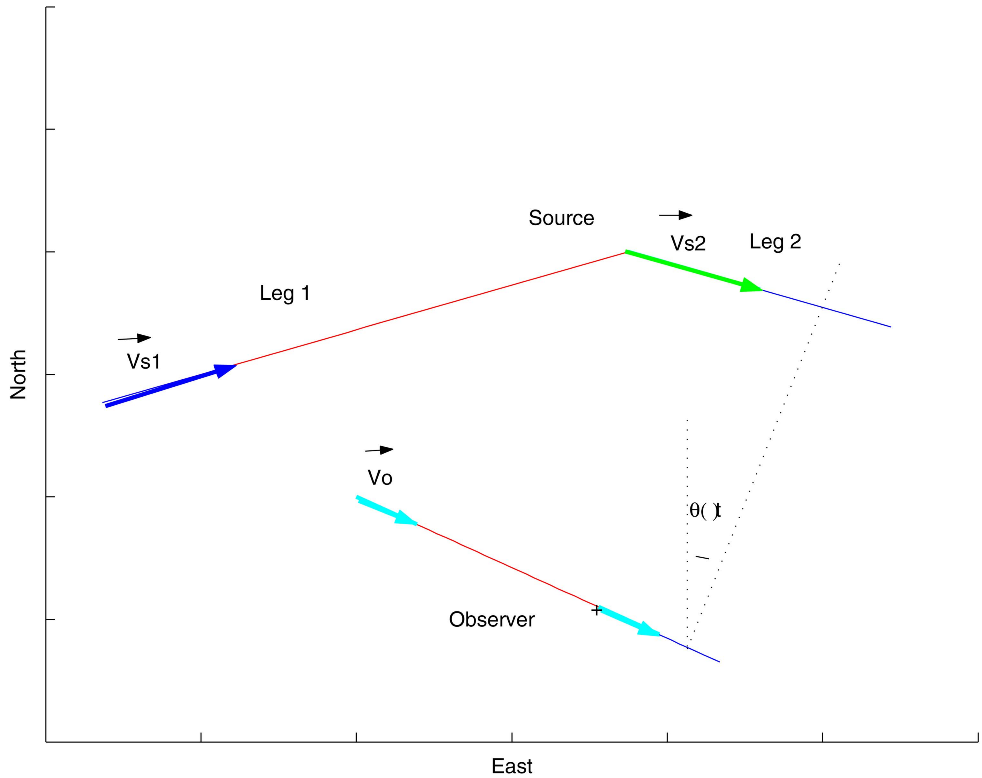

Fig. 5. Example of observer and source trajectories composed by two legs.

and the corresponding leg-by-leg BOMTMA $\tilde{Z} = [\tilde{x}_S(t_K)\ \tilde{y}_S(t_K)\ \tilde{v}_S\ \tilde{c}_{S,1}\ \tilde{c}_{S,2}]^{\mathrm{T}}$, with

$$[\tilde{x}_S(t_K)\quad \tilde{y}_S(t_K)]^{\mathrm{T}} = [\tilde{x}_2\quad \tilde{y}_2]^{\mathrm{T}}$$

$$\tilde{v}_S = \sqrt{\tilde{\dot{x}}_2^2 + \tilde{\dot{y}}_2^2}$$

$$\tilde{c}_{S,1} = \operatorname{atan}\left(\frac{\tilde{\dot{x}}_1}{\tilde{\dot{y}}_1}\right)$$

$$\tilde{c}_{S,2} = \operatorname{atan}\left(\frac{\tilde{\dot{x}}_2}{\tilde{\dot{y}}_2}\right).$$

REMARK by construction, $\tilde{x}_1 = \tilde{x}_2$ and $\sqrt{\tilde{\dot{x}}_1^2 + \tilde{\dot{y}}_1^2} = \sqrt{\tilde{\dot{x}}_2^2 + \tilde{\dot{y}}_2^2}$, but there is no reason that $\tilde{y}_1 = \tilde{y}_2$. So, another solution must be $[\tilde{x}_S(t_K)\ \tilde{y}_S(t_K)]^{\mathrm{T}} = [\tilde{x}_2\ \tilde{y}_1]^{\mathrm{T}}$.

3.2. Problem Formulation

A 500-run Monte Carlo simulation allows the behavior of this new estimator to be appreciated. To compare the MLE BOMTMA estimate $\hat{Z}$ and the leg-by-leg BOMTMA estimate $\tilde{Z}$, we use the scenario presented in [7] which is illustrated in Fig. 6: let us recall that the observer starts from the origin with a speed of 5 m/s and a heading of 90°. Meanwhile, the source, with a speed of 4 m/s, starts its trajectory at $[0\ \mathrm{km}, 10\ \mathrm{km}]^{\mathrm{T}}$ with an initial heading of 90°. At time $t_M = 20$ min, it suddenly changes its course and its new heading is 240°. The total duration of the scenario is 30 min corresponding to 450 measurements (the sampling time is $\Delta t = 4$ s). The standard deviation of the measurement noise is 1°.

The average values of the coordinates of the two estimates, their respective biases and their empirical standard deviations are given in Table I. They are compared to the true vector and the minimum standard deviations deduced from the CRLB.

We observe an increase in the bias and the standard deviation, but the quality of the leg-by-leg BOMTMA estimator is only weakly degraded. Moreover, the computation time of the leg-by-leg BOMTMA estimator is 2.5 times less than the BOMTMA computation time. A compromise can probably be found: the leg-by-leg estimate can be used as an initial point for the BOMTMA numerical routine. It will reduce the risk of stalling at a local minimum. Fig. 7 shows the 500 estimates together with the 90% confidence ellipsoid deduced from the CRLB.

4. COMPARISON OF THE RESPECTIVE PERFORMANCES OF THE BOMTMA AND THE CONVENTIONAL BOTMA

One can ask a relevant question concerning tactical aspects: do situations exist in which the performance of the BOMTMA is superior to the performance of the BOTMA in terms of estimated range accuracy, assuming that the antennas are the same?

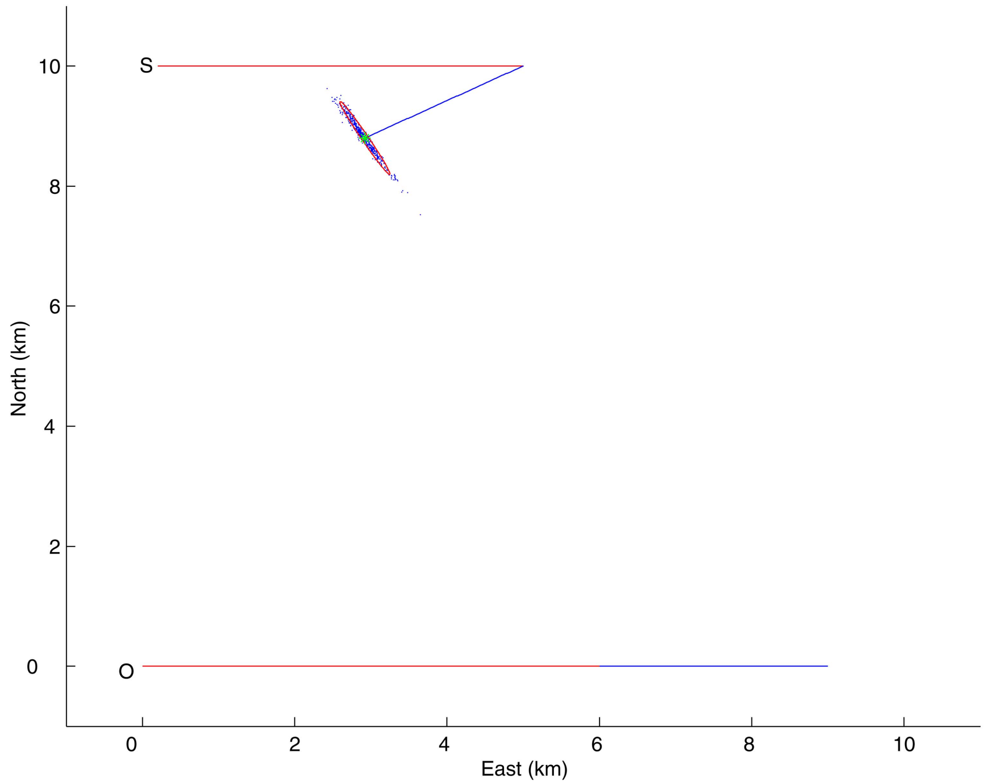

Fig. 6. 500 MLE BOMTMA estimates of the final position.

TABLE I
Comparison of Performances of the Two Estimators

Z_K	Units	$Z_{K,\text{True}}$	Average of $\hat{Z}_K$	Average of $\tilde{Z}_K$	Bias of $\hat{Z}$	Bias of $\tilde{Z}$	σ_{CRLB}	$\hat{\sigma}$ of $\hat{Z}$	$\tilde{\sigma}$ of $\tilde{Z}$
$x_S(t_K)$	km	2.921	2.897	**2.872**	0.024	**0.049**	0.153	0.175	**0.213**
$y_S(t_K)$	km	8.800	8.828	**8.875**	0.028	**0.075**	0.283	0.308	**0.364**
v_S	m/s	4	4.10	**4.10**	0.10	**0.10**	0.03	0.13	**0.17**
$c_{S,1}$	degree	90	90.5	**89.4**	0.5	**0.6**	12	12	**13**
$c_{S,2}$	degree	240	240	**241**	0	**1**	7.5	7	**9**

For the conventional BOTMA, the observer must correctly maneuver and it has to estimate a 4-dimensional state vector [13], whereas for the BOMTMA, the observer does not maneuver but it has to estimate a 5-dimensional vector. Because the number of unknown is less in BOTMA than in BOMTMA, one can think that the BOMTMA returns a less accurate estimated range than the BOTMA. Surprisingly, for some scenarios, this statement is wrong. We give three examples: the first one contradicts the intuition; for the second, the performances are similar, and the last is an example of the superiority of the BOTMA to the BOMTMA.

We consider two mobiles: one maneuvers (denoted hereafter by the letter "M") and the second (denoted "N") does not. Each of them performs a TMA against the other.

For each example, the speeds of M and N are 4 m/s and 5 m/s, respectively. The heading of the non-maneuvering platform is equal to 90 degrees. The kinds of maneuvering source trajectory have been chosen: a "surrounding" trajectory (see Fig. 8(a)) and two "escaping" trajectories (see Figs. 9(a) and 10(a)). The total duration is 30 min. The maneuvering platform changes its course at 15 min. At this time, its location is aligned with the course of the observer.

The bearings, collected at a sample time of 4 seconds by each platform, are corrupted by an additive Gaussian noise with the same standard deviation equal to 1 degree. We have computed the relative accuracy of the estimated range (at the final time t_K) by the mean of the CRLB: In $\sigma_{\rho(t_K)}/\rho(t_K)$, given in percentage, $\sigma_{\rho(t_K)}$ is the CRLB of the estimated final range.

Typical scenarios are plotted in Figs. 8, 9 and 10, ("M" and "N" give the initial positions of the two platforms) together with the corresponding $\sigma_{\rho(t_K)}/\rho(t_K)$ vs. $\rho(t_K)$. In these figures, the lines joining circles are related to the conventional BOTMA and the lines joining the "+" are for the BOMTMA. We have changed the final range by modifying the initial position of the non-maneuvering platform along the x-axis.

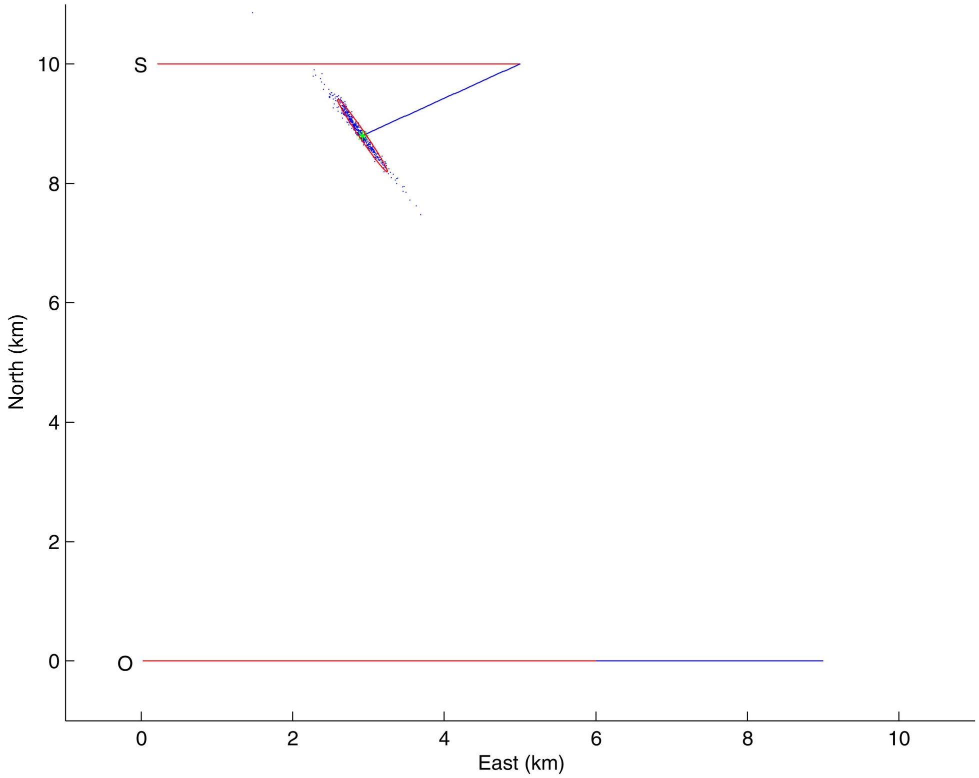

Fig. 7. 500 leg-by-leg BOMTMA estimates of the final position.

EXAMPLE 1 In this scenario, the first and the second headings of the maneuvering source are respectively $-135°$ and $135°$.

EXAMPLE 2 The first and the second headings of the maneuvering source are respectively $135°$ and $-135°$.

EXAMPLE 3 The first and the second headings of the maneuvering source are respectively $-135°$ and $135°$.

5. CONCLUSIONS

We have presented the problem of bearing-only target motion analysis when neither the source nor the observer maneuvers. This yields the so called partial BOTMA, since the observability is missing. Then, we have proposed another estimate for a two-leg source trajectory by bearings-only TMA from a non-maneuvering observer, which is an alternative solution of the maximum likelihood estimate proposed in [7]. The computation time is reduced by a factor of approximately 2.5. The price is a small degradation in the statistical performance. We have also shown, by three examples, that the superiority of the BOTMA to the BOMTMA is not always guaranteed.

Further work will be carried out to extend this estimation principle (leg-by-leg estimates, then fusion of them) to the case of several legs. Robustness to the assumption of constant speed and of the immediate change of heading will be the topic of another paper [8].

But the challenge remains to construct a powerful test to detect the maneuver of the source.

APPENDIX. COMPUTATION OF THE CONFIDENCE BANDS

To conduct properly the computation, we need to define the following vector $\tilde{X} = [y \ \ \dot{x} \ \ \dot{y}]^{\mathrm{T}}$ whose components are the last there components of X (defined in Subsection 2.4). We rename the components of $\tilde{X}$ as follows: $\tilde{X} = [x_1 \ \ x_2 \ \ x_3]^{\mathrm{T}}$ for convenience and we define the function

$$\theta_k(\tilde{X}) = \operatorname{atan}\left[\frac{\bar{\rho}\sin\beta_{t^*} + (t_k - t^*)(x_2 - \dot{x}_O)}{x_1 - y_O(t^*) + (t_k - t^*)(x_3 - \dot{y}_O)}\right]$$

which would be the noise-free bearing of a source at time t_k, whose trajectory would be defined by X.

Under classic Gaussian assumption about the additive noise, the Fisher information matrix is

$$F(\tilde{X}) = \sum_{k=1}^{K} \frac{1}{\sigma_k^2} \nabla_{\tilde{X}}\theta_k(\tilde{X})\nabla_{\tilde{X}}^{\mathrm{T}}\theta_k(\tilde{X})$$

and the CRLB of $\tilde{X}$ is $B(\tilde{X}) = F(\tilde{X})^{-1}$.

We go into detail about the expression of $\nabla_{\tilde{X}}\theta_k(\tilde{X})$ by defining the following quantities

$$\Delta_t(t_k) = t_k - t^*$$

$$\Delta_x(t_k) = \bar{\rho}\sin\beta_{t^*} + \Delta_t(t_k)(x_2 - \dot{x}_O),$$

$$\Delta_y(t_k) = x_1 - y_O(t^*) + \Delta_t(t_k)(x_3 - \dot{y}_O),$$

$$r(t_k) = \sqrt{\Delta_x^2(t_k) + \Delta_y^2(t_k)}.$$

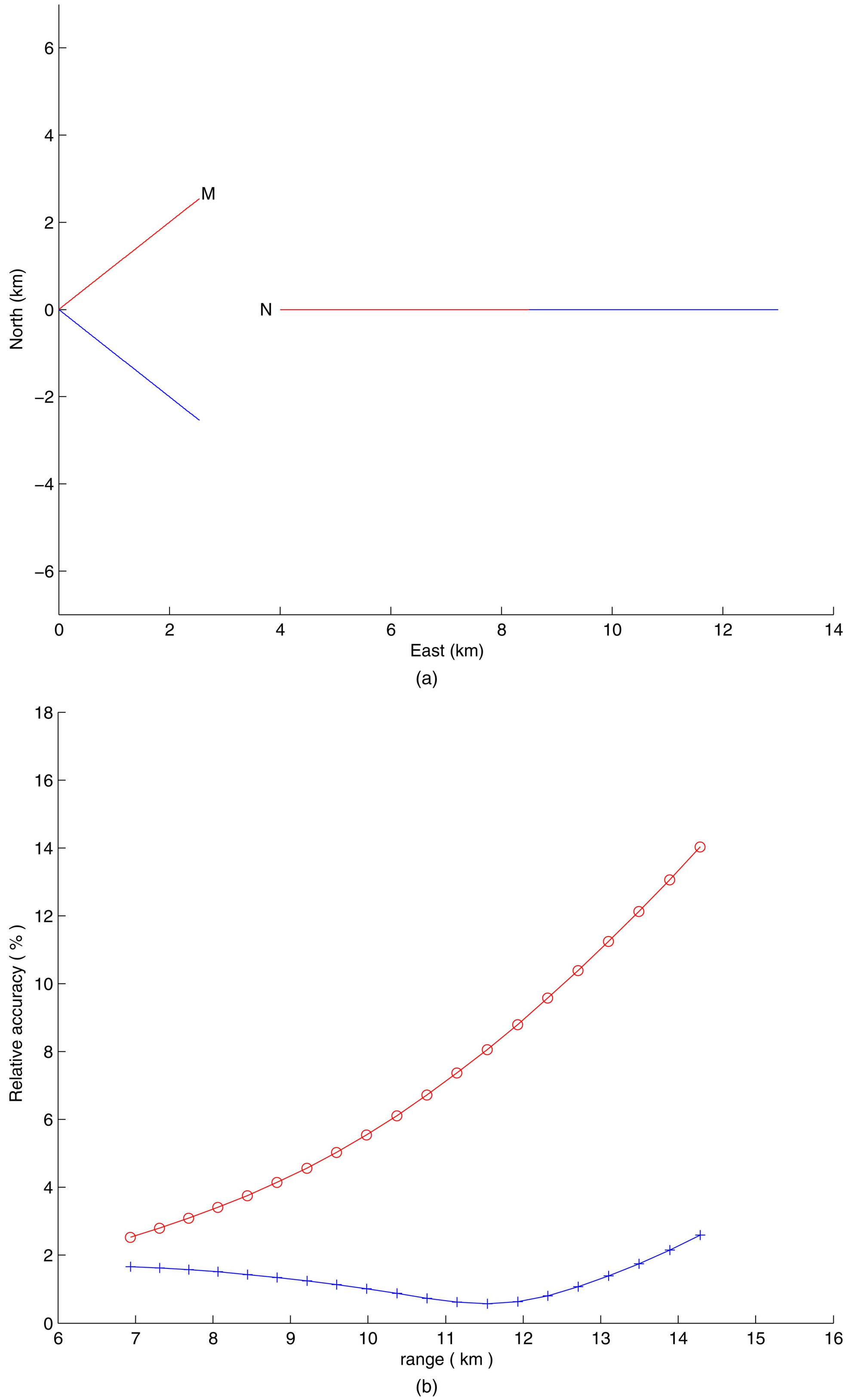

Fig. 8. (a) Typical surrounding maneuvering platform trajectory for Example 1. (b) The relative accuracies of the estimated ranges for the first example ("o" for the conventional BOTMA, "+" for the BOMTMA).

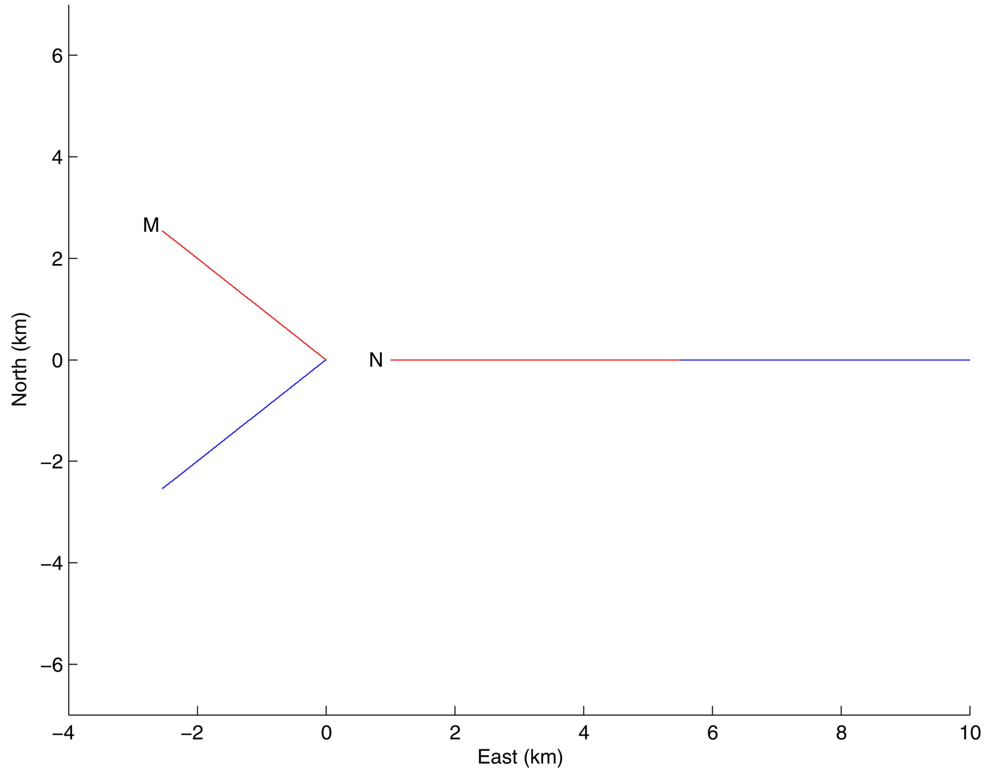

(a)

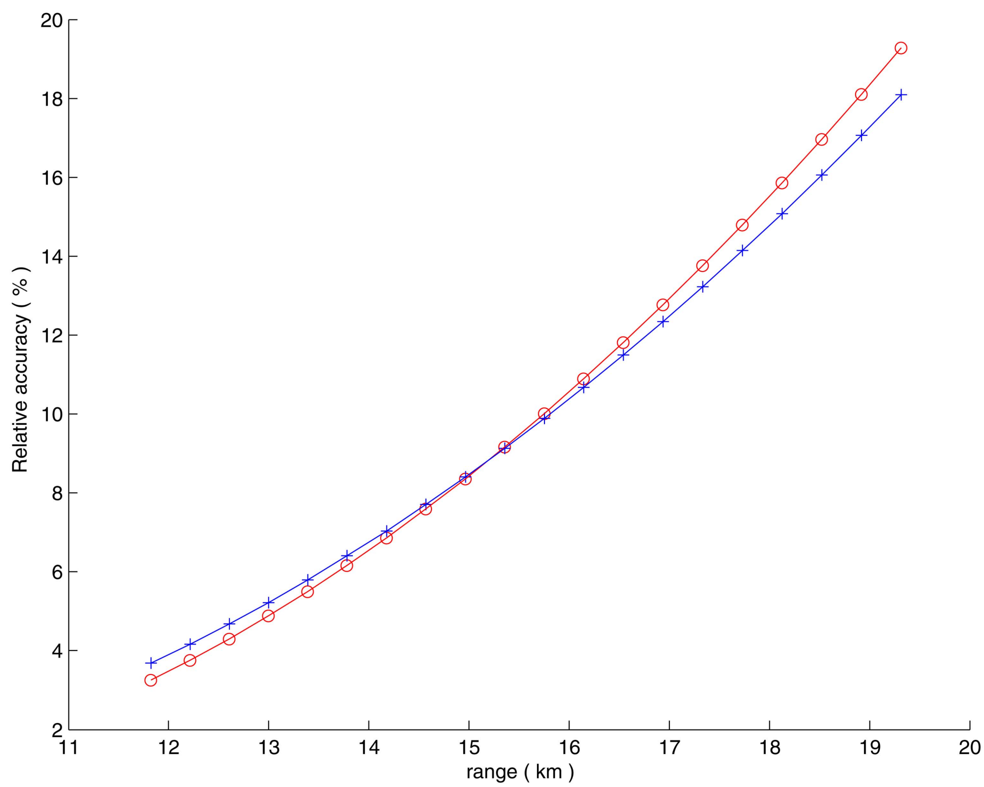

(b)

Fig. 9. (a) Typical escaping maneuvering platform for the second example. (b) The relative accuracies of the estimated ranges for the second example ("o" for the conventional BOTMA, "+" for the BOMTMA).

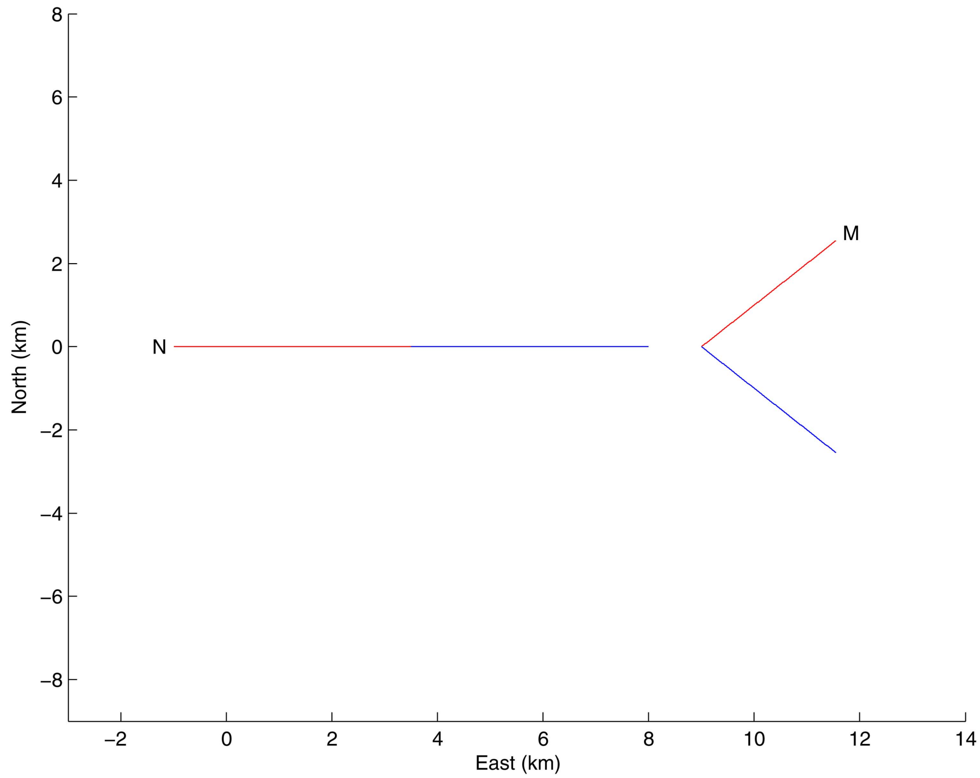

(a)

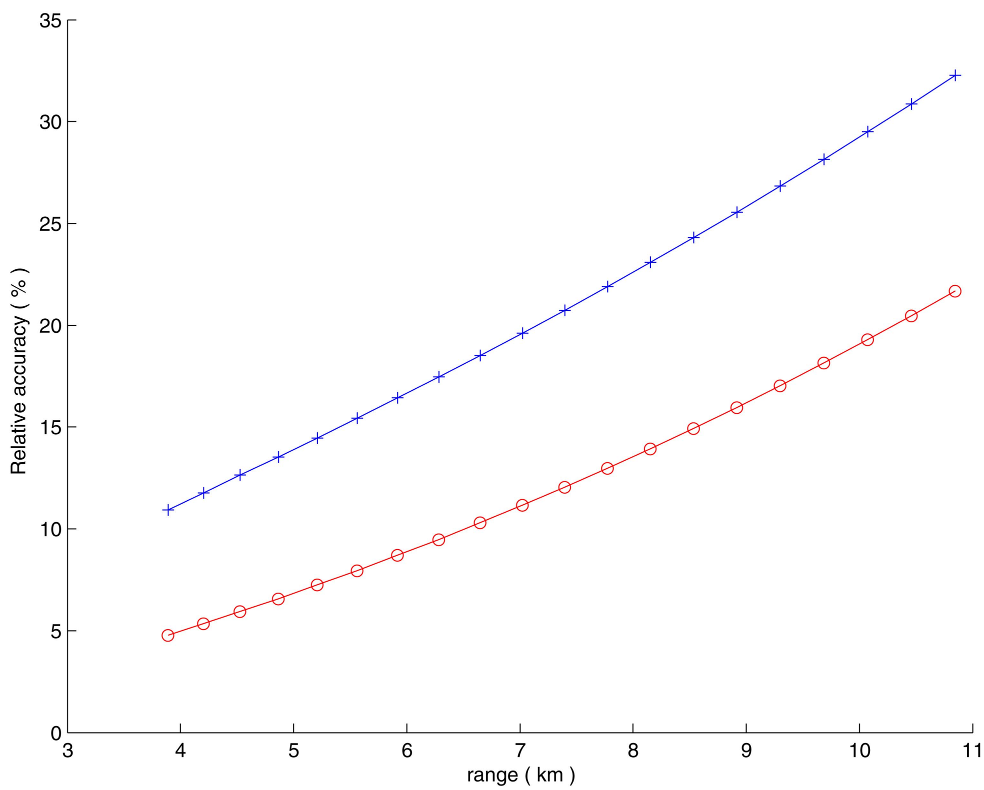

(b)

Fig. 10. (a) Typical escaping maneuvering platform trajectory for the third example. (b) The relative accuracies of the estimated ranges for the third example ("o" for the conventional BOTMA, "+" for the BOMTMA).

We deduce that

$$\nabla_{\tilde{X}}\theta_k(\tilde{X}) = \frac{1}{r^2(t_k)}\begin{bmatrix} -\Delta_x(t_k) \\ \Delta_t(t_k)\Delta_y(t_k) \\ -\Delta_t(t_k)\Delta_x(t_k) \end{bmatrix}.$$

The computation of the confidence bands is based on the Jacobians of the two following mappings

$$\tilde{X} = \begin{bmatrix} x_1 \\ x_2 \\ x_3 \end{bmatrix} \mapsto Y = \begin{bmatrix} y_1 \\ y_2 \\ y_3 \end{bmatrix} \mapsto V(\rho) = \begin{bmatrix} v(\rho) \\ c(\rho) \end{bmatrix},$$

with

$$Y = \begin{bmatrix} \operatorname{atan}\left[\dfrac{\bar{\rho}\sin\beta_{t^*}}{x_2 - y_O(t^*)}\right] \\ \dfrac{\sqrt{(x_3 - \dot{x}_O)^2 + (x_4 - \dot{y}_O)^2}}{\sqrt{(\bar{\rho}\sin\beta_{t^*})^2 + [x_2 - y_O(t^*)]^2}} \\ \operatorname{atan}\left[\dfrac{x_3 - \dot{x}_O}{x_4 - \dot{y}_O}\right] \end{bmatrix} \quad \text{and}$$

$$V(\rho) = \begin{bmatrix} v(\rho) = \sqrt{(\rho y_2 \sin y_3 + \dot{x}_O)^2 + (\rho y_2 \cos y_3 + \dot{y}_O)^2} \\ c(\rho) = \operatorname{atan}\left[\dfrac{\rho y_2 \sin y_3 + \dot{x}_O}{\rho y_2 \cos y_3 + \dot{y}_O}\right] \end{bmatrix}.$$

The CRLB of $V(\rho)$ is then

$$B(V(\rho)) = J_2 J_1 B(\tilde{X}) J_1^{\mathrm{T}} J_2^{\mathrm{T}}$$

where J_1 is the Jacobian of the mapping $\tilde{X} \mapsto Y$ and J_2 is the Jacobian of the mapping $Y \mapsto V(\rho)$. We evaluate the confidence bands of each component of $v(\rho)$ and of $c(\rho)$ from the diagonal terms of $B(V(\rho))$.

ACKNOWLEDGMENT

We are grateful to Caroline Turner for having upgraded the writing of this paper.

REFERENCES

[1] Y. Bar-Shalom and X. R. Li
Estimation and Tracking: Principles, Techniques, and Software.
Artech House (1993).

[2] P. Blanc-Benon and J. M. Passerieux
Fusion of reduced-rank TMA estimates.
IEEE Transactions on Aerospace and Electronic Systems, **AES-36**, 3 (July 2000), 750–759.

[3] J. E. Dennis
A user's guide to nonlinear optimization algorithms.
In *Proceedings of IEEE*, **72**, 12 (Dec. 1984).

[4] K. C. Ho and Y. T. Chan
An asymptotically unbiased estimator for bearings-only and Doppler-bearing target motion analysis.
IEEE Transactions on Signal Processing, **54**, 3 (Mar. 2006), 809–821.

[5] J. Holst and A. Holtsberg
On target manoeuvres in bearings-only tracking.
In *Proceedings of the 25th Asilomar Conference on Circuits Systems*, (Nov. 1991).

[6] C. Jauffret and D. Pillon
Observability in passive target motion analysis.
IEEE Transactions on Aerospace and Electronic Systems, **AES-32**, 4 (Oct. 1996), 1290–1300.

[7] C. Jauffret, D. Pillon, and A. C. Pignol
Bearings-only TMA without observer maneuver.
In *Proceedings of the 11th International Conference on Information Fusion*, Cologne, Germany, (July 2008), 501–508.

[8] C. Jauffret, D. Pillon, and A. C. Pignol
Bearings-only maneuvering target motion analysis from a non maneuvering platform.
IEEE Transactions on Aerospace and Electronic Systems, **AES-46**, 4 (Oct. 2010), 1934–1949.

[9] C. Jauffret, D. Pillon, and A. C. Pignol
Leg-by-leg bearings-only TMA without observer maneuver.
In *Proceedings of the 12th International Conference on Information Fusion*, Seattle, (July 2009), 2036–2043.

[10] J. P. Le Cadre and C. Jauffret
Discrete-time observability and estimability analysis for bearings-only target motion analysis.
IEEE Transactions on Aerospace and Electronic Systems, **AES-33**, 1 (Jan. 1997), 178–201.

[11] J. P. Le Cadre and S. Laurent-Michel
Optimizing the receiver maneuvers for bearings-only tracking.
Automatica, **35** (1999), 591–606.

[12] S. C. Nardone and V. J. Aidala
Observability criteria for bearings-only target motion analysis.
IEEE Transactions on Aerospace and Electronic Systems, **AES-17**, 2 (Mar. 1981), 162–166.

[13] S. C. Nardone, A. G. Lindgren, and K. F. Gong
Fundamental properties and performance of conventional bearings-only target motion analysis.
IEEE Transactions on Automatic Control, **AC-29**, 9 (Sept. 1984), 775–787.

[14] S. C. Nardone and M. L. Graham
A closed-form solution to bearings-only target motion analysis.
IEEE Journal of Oceanic Engineering, **OE-22**, 1 (Jan. 1997), 168–178.

[15] J. M. Passerieux and D. Van Cappel
Optimal observer maneuver for bearings-only tracking.
IEEE Transactions on Aerospace and Electronic Systems, **AES-34**, 3 (July 1998), 777–788.

[16] D. T. Pham
Some quick and efficient methods for bearings-only target motion analysis.
IEEE Transactions on Signal Processing, **SP-41**, 9 (Sept. 1993), 2737–2751.

[17] J. Ru, V. P. Jilkov, X. R. Li, and A. Bashi
Detection of target maneuver onset.
IEEE Transactions on Aerospace and Electronic Systems, **AES-45**, 2 (Apr. 2009), 536–554.

Claude Jauffret born in France on March 29, 1957, received the diplôme d'Etudes Appronfondies in applied mathematics from Saint Charles University, Marseille, France, in 1981, the Diplôme d'Ingénieur from Ecole Nationale Supérieure d'Informatique et de Mathématiques Appliqués de Grenoble, Grenoble, France, in 1983, the title of Docteur de l'Université in 1993 and the Habilitation à Diriger des Recherches from the Université de Toulon et du Var, France.

From November 1983 to November 1988, he worked on passive sonar systems, more precisely on target motion analysis at GERDSM, France. After a sabbatical year at the University of Connecticut (from November 1988 to December 1989) during which he worked of tracking problems in cluttered environment, he developed researches in tracking, data fusion, and extraction in CERDSM. Since September 1996, he has been at the Université de Toulon et du Var where he teaches statistical signal processing. His current researches are about observability, estimation in non linear systems as they appear in tracking problems.

He is an associate editor for *IEEE Transactions on Aerospace and Electronic Systems.*

Denis Pillon comes from a small French mountain called "Le Jura." He received the Diplôme d'Ingénieur from Ecole Supérieure de Physique et de Chimie Industrielle (ESPCI-Paris) in 1977 and the Diplôme d'Etudes Approfondies in probability theory from the Jussieu University, Paris in 1977.

From 1978 to 1979 he worked in the area of operational research at the Centre InterArmées de Recherche Opérationnelle (CIRO) agency of the ministère de la Défense. Since 1980 he has been employed by Thomson Compagny (now Thales Compagny), France. From 1980 to 1981 he worked on sonar array processing. From 1982 to 1986, he was consultant at the GERDSM for which he worked on sea trial analysis and TMA. From 1987 to 1989, he worked on tracking and track clustering and in 1990 he was appointed group leader of signal and data processing laboratory at Thomson Sintra company, Sophia Antipolis, France. From 1992 to 1999, he was consultant at the DCN sonar laboratory. He worked on new sonar arrays and various submarine combat systems. Since 2000, he has been sonar expert at Thales Underwater Systems (Sophia-Antipolis). His current researches are about passive sonar performances estimation, submarine and torpedo array processing, and long term prospective studies for submarine warfare.

Annie-Claude Pignol born in France on November 10, 1965, received the Diplôme d'Etudes Appronfondies in optics and image processing from the Université de Toulon et du Var, Toulon, France, in 1988 and the title of Docteur de l'Université in 1991 from the Université de Toulon et du Var, France.

Since September 1994, she has been at the Université de Toulon et du Var where she teaches electronic systems. Her researches were focused signal processing applied to biomedical systems before turning them to Target Motion Analysis.